Simultaneous computation of free energies and kinetics of rare events

Daniele Moroni,[1] Titus S. van Erp,[2] and Peter G. Bolhuis[1]
[1]*van 't Hoff Institute for Molecular Sciences, Universiteit van Amsterdam, Nieuwe Achtergracht 166, 1018 WV Amsterdam, The Netherlands*
[2]*Laboratoire de Physique/Centre Européen de Calcul Atomique et Moléculaire, Ecole Normale Supérieure de Lyon, 46 allée d'Italie, 69364 Lyon Cedex 07, France*
(Received 11 October 2004; published 31 May 2005)

We introduce a method to evaluate simultaneously the reaction rate constant and the free energy profile of a process in a complex environment. The method employs the partial path transition interface sampling technique we recently developed for the calculation of rate constants in diffusive systems. We illustrate the applicability of the technique by studying a simple dimer in a repulsive fluid, and show that the free energy can be obtained at no additional computational cost.

DOI: 10.1103/PhysRevE.71.056709 PACS number(s): 82.20.Pm, 02.70.−c, 05.20.Gg, 82.20.Wt

I. INTRODUCTION

The calculation of kinetic information (e.g., rate constants) of rare-event-dominated processes such as protein folding, chemical reactions in solution, and crystal nucleation remains, in general, one of the great computational challenges. Application of straightforward molecular dynamics (MD) would in principle yield all atomistic kinetic information. However, MD requires a sufficiently small time step to describe the elementary molecular motion, while a reactive process usually exceeds this molecular time scale by many orders of magnitude. As a result, the calculation of rates using MD is for most systems beyond the reach of present computers. To enable the study of the kinetics for processes in which a high free energy barrier separates the stable states, the Bennett-Chandler method [1,2] writes the rate constant as a product of two factors: the equilibrium probability to be on the barrier, and a kinetic prefactor. The first factor is given by the free energy difference between the transition state region and the stable state as a function of a reaction coordinate. The concept of free energy is to reduce the myriad degrees of freedom to a single or a set of variables that are able to describe the reaction process. The numerical computation of free energy profiles or landscapes has proved invaluable for gaining insight in complex processes, and many different methods have been developed [3]. For instance, in the widely used umbrella sampling (US) technique one biases the system into the low probability (or high free energy) regions to gain more statistics [3]. Although US gives the free energy barrier, it is not sufficient for the rate constant. Therefore, the second step in the Bennett-Chandler procedure is the calculation of a dynamical correction factor called the transmission coefficient by starting many MD trajectories from the top of the barrier. Unfortunately, when the reaction coordinate fails to capture the molecular mechanism, this procedure becomes very inefficient due to the small value of the transmission coefficient. Only when the reaction coordinate is correctly chosen (and is therefore considered as a "true reaction coordinate"), the phase space region on top of the barrier corresponds to the transition state dividing surface and, hence, the transmission coefficient will have reasonable value that can be computed.

For this reason, Chandler and co-workers developed transition path sampling (TPS), a method that obtains the kinetics of a complex rare event process without prior knowledge of the reaction coordinate, but just using an order parameter able to distinguish the initial and final states [4]. TPS gathers a collection of reactive pathways connecting the initial and final regions by employing a random walk in trajectory space based on the Monte Carlo (MC) shooting move [4]. Based on this, we recently developed a more efficient transition interface sampling (TIS) method [5], which has shown to be a promising tool for the calculation of rate constants between two stable states in high dimensional complex systems separated by large free energy barriers [6]. For diffusive systems we also devised a variation of this method, called partial path TIS (PPTIS) [7], effectively exploiting the loss of long time correlation. In PPTIS the paths do not have to go all the way to the initial or final state, thus greatly improving efficiency.

TIS and PPTIS no longer use the free energy, but the crossing probability function whose calculation is much less sensitive to the problem of the right reaction coordinate [5,7]. However, for the analysis of complex and diffusive processes, e.g., conformational changes of biomolecules, it could be useful to have, besides the crossing probabilities and the rate constants, also the free energy profile along order parameters, for instance to identify metastable states and bottlenecks in the mechanism.

In this article we show how to obtain the free energy landscape *together with* the rate constants in one single simulation series using PPTIS concepts.

II. THEORY

Consider a complex system which undergoes a transition between two stable states A and B, separated by a high barrier, but with a reasonably flat and broad plateau. Due to the height of the barrier the population on top will be very small, yielding exponential two-state behavior and a well defined rate constant. In addition, as this barrier in not sharply peaked, but has this broad plateau, the transitions will have a strong diffusive character and it is therefore often referred to as a diffusive barrier. The PPTIS method requires a set of

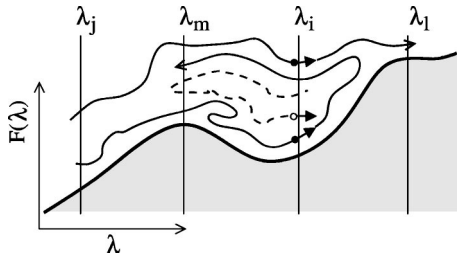

FIG. 1. Illustration of the conditional crossing probability $P(^{l}_{m}|^{i}_{j})$ for a certain configuration of interfaces $\lambda_i, \lambda_j, \lambda_l$, and λ_m along a free energy barrier. The condition $|^{i}_{j})$ restricts the set of phase points to those that cross interface λ_i in one time step (in the limit $dt \to 0$ this corresponds to a collection of phase points on the surface λ_i, but with a weight proportional to $\dot{\lambda}$) and its backward trajectory should cross λ_j before λ_i. In this picture only the black solid circles satisfy this condition. The forward evolution is associated with $(^{l}_{m}|$ and measures whether interface λ_l is crossed before λ_m (as in the upper path) or not (as in the lower one). The fraction that crosses λ_l before λ_m yields $P(^{l}_{m}|^{i}_{j})$.

$n+1$ nonintersecting multidimensional interfaces $\{0,1,\ldots,n\}$ described by an order parameter $\lambda(x)$ function of the system phase point x, i.e., of all positions and velocities. This order parameter should be able to describe the stable states, but does not have to correspond to the true reaction coordinate or, equivalently, none of the surfaces have to be close to the true transition dividing surface.

We choose λ_i, $i=0,\ldots,n$, such that $\lambda_{i-1}<\lambda_i$, and that the boundaries of states A and B are described by λ_0 and λ_n, respectively. Now consider a deterministic Hamiltonian trajectory x_t of arbitrary length, where x_t is the complete phase space vector at a time t. We define the conditional crossing probability $P(^{l}_{m}|^{i}_{j})$ as the probability for a trajectory x_t to reach interface l before m under the condition that it crosses at $t=0$ interface i, while coming directly from interface j in the past. Directly means without crossing interface i another time (see Fig. 1). These probabilities $P(^{l}_{m}|^{i}_{j})$ are defined on any set of four interfaces. Of special interest are the so-called long distance crossing probabilities $P_i^+ \equiv P(^{i}_{0}|^{1}_{0})$ and $P_i^- \equiv P(^{0}_{i}|^{i-1}_{i})$. The forward and backward rate constants of the A to B transition can be written as

$$k_{AB} = f_A P_n^+, \quad k_{BA} = f_B P_n^-, \tag{1}$$

where we assumed that once the system has switched to the other state, the chance of recrossing has vanished. The factors f_A and f_B are the fluxes out of A and B, respectively, and can be calculated accurately by counting the frequency of leaving A and B using straightforward MD. The other factors P_n^+ and P_n^- can be calculated in a TIS simulation. However, in case there is memory loss between the interfaces, we can approximate the long distance crossing probabilities by the recursive relations

$$P_j^+ \approx \frac{p_{j-1}^{\pm} P_{j-1}^+}{p_{j-1}^{\pm} + p_{j-1}^{=} P_{j-1}^-}, \quad P_j^- \approx \frac{p_{j-1}^{\mp} P_{j-1}^-}{p_{j-1}^{\pm} + p_{j-1}^{=} P_{j-1}^-}, \tag{2}$$

in which the one-interface-crossing probabilities are defined as $p_i^{\pm} \equiv P(^{i+1}_{i-1}|^{i}_{i-1})$, $p_i^{\mp} \equiv P(^{i-1}_{i+1}|^{i}_{i+1})$, $p_i^{=} \equiv P(^{i-1}_{i+1}|^{i}_{i-1})$, and $p_i^{\pm} \equiv P(^{i+1}_{i-1}|^{i}_{i+1})$. Starting with $P_1^+ = P_1^- = 1$, we can iteratively determine (P_j^+, P_j^-) for $j=2,\ldots,n$. The one-hopping probabilities are calculated employing the shooting algorithm [4]. Because of the memory loss assumption, the PPTIS expression essentially transforms the rate equation into a Markovian hopping sequence. Yet, if the dynamics is diffusive and the interfaces are sufficient far apart, the recursive expression (2) is an excellent approximation [7]. A similar method to PPTIS is the *milestoning* method of Faradjian and Elber [8]. The two methods are very similar, but differ on two crucial points. The milestoning method assumes a complete loss of memory at each interface. Hence, at each interface the system can hop either to the right or to the left with a certain probability and these probabilities do not depend on the history of the path. PPTIS takes a stronger history dependence into account. At each interface memory effects may persist but not much longer than the time needed to travel from one interface to the other. Recent PPTIS calculations on crystal nucleation have shown that this stronger history dependence is probably important for realistic systems [9]. On the other hand, the milestoning approach puts more effort into describing the time evolution on the barrier by using time dependent hopping probabilities. These are required if one wants to study, for instance, the decay of a distribution that is initially out of equilibrium, or the diffusion behavior on the barrier. This time aspect introduces another history dependence [8], which is absent in PPTIS where the final crossing probability is a quantity independent of time. This is justified by the fact that PPTIS always assumes that the barrier is sparsely populated. Hence, the time that the system spends on the barrier can be long from a computational perspective, but is still negligible compared to the expected time the system needs to enter the barrier plateau region from one of the stable states. In principle, this condition should always be satisfied for a system that shows exponential decay and, hence, has a well defined rate, but, of course, systems that do not obey these conditions can still be interesting to study. To summarize, both methods are very similar, but each one is more accurate in one of the points described above. However, the two aspects do not exclude each other and could easily be merged into a single algorithm if needed.

In addition to the rate constant, it is also possible to obtain the equilibrium free energy profiles along λ. For that we need to calculate the probability $P(\lambda)$ to find the system at a certain value of λ. In principle, if we perform path sampling between two interfaces, and allow the path to be completely free, but stop integrating when an interface is hit, we essentially perform umbrella sampling between the interfaces using hybrid MC methods [10]. In that case, simply measuring the probability along the paths to be at a value of λ and joining all histograms would suffice to obtain the entire free energy $\beta F(\lambda) \equiv -\ln P(\lambda)$. The PPTIS ensembles have a strong resemblance to US where the interfaces act as hard window boundaries. However, the PPTIS method introduces a bias, by restricting all paths in the ensemble to cross the middle interface. The λ_i path ensemble in the PPTIS formalism consists of all possible paths that start and end at either λ_{i-1} or λ_{i+1} and have at least one crossing with λ_i. Similar to TPS [4], we consider a path as a time-discretized sequence of

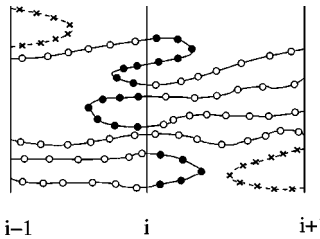

FIG. 2. Illustration of *loop* and *boundary* points. The open circles denote boundary points with $b_i(x)=1$, time slices that hit a boundary in one time direction and reach λ_i in the opposite time direction. The loop points (full circles) with $l_i(x)=1$ meet first the middle interface in both directions. For both loop and boundary points $w_i(x)=1$. The dashed lines are paths that do not belong to the ensemble as they do not cross λ_i. Hence, the corresponding time slices (crosses) are not part of the subset of phase points counted in the λ_i ensemble [thus $w_i(x)=0$], but are loop points of the neighboring interfaces.

phase points, called time slices. The collection of all time slices of these paths is a subset of the phase space points confined between λ_{i-1} and λ_{i+1} because we are missing the points around the outer interfaces, as shown in Fig. 2. We can correct for this by comparing neighboring interface ensembles. For this purpose, it is convenient to categorize the time slices into the *loop* type and *boundary* type of phase points as illustrated in Fig. 2. We define $h_{i,j}^{f(b)}(x)$ to be 1 if the forward (backward) deterministic trajectory starting from phase space point x meets λ_i before λ_j and 0 otherwise. We can now define the loop and boundary characteristic functions as $l_i(x)=h_{i,i-1}^f(x)h_{i,i+1}^f(x)h_{i,i-1}^b(x)h_{i,i+1}^b(x)$ and $b_i(x)=h_{i-1,i}^f(x)h_{i,i-1}^b(x)+h_{i-1,i}^b(x)h_{i,i-1}^f(x)+h_{i+1,i}^f(x)h_{i,i+1}^b(x)+h_{i+1,i}^b(x)h_{i,i+1}^f(x)$. Again, these functions are either one or zero depending on whether x belongs to its loop or boundary category. Similarly, the complete set of time slices in the PPTIS ensemble can be characterized by $w_i(x)=l_i(x)+b_i(x)$. This function is one, when the phase belongs to a path in the PPTIS λ_i ensemble. Otherwise it is zero. As b_i and l_i vanish whenever w_i is zero,

$$b_i(x)w_i(x)=b_i(x) \text{ and } l_i(x)w_i(x)=l_i(x), \tag{3}$$

for any phase point x. Moreover, for a phase point with $\lambda_{i-1}<\lambda(x)<\lambda_i$ it also holds that

$$b_{i-1}(x)=b_i(x),$$

$$\begin{aligned} l_{i-1}(x)+b_{i-1}(x)+l_i(x)&=w_{i-1}(x)+l_i(x)=l_{i-1}(x)+b_i(x)+l_i(x)\\ &=l_{i-1}(x)+w_i(x)=1. \end{aligned} \tag{4}$$

Using these equations for any $\lambda', \lambda_{i-1}<\lambda'<\lambda_i$,

$$\begin{aligned} P(\lambda')&=\langle\delta(\lambda(x)-\lambda')\rangle=\langle\delta(\lambda(x)-\lambda')[w_{i-1}(x)+l_i(x)]\rangle\\ &=\langle\delta(\lambda(x)-\lambda')w_{i-1}(x)\rangle+\langle\delta(\lambda(x)-\lambda')l_i(x)\rangle\\ &=\langle w_{i-1}(x)\rangle\langle\delta(\lambda(x)-\lambda')\rangle_{w_{i-1}}\\ &\quad+\langle w_i(x)\rangle\langle\delta(\lambda(x)-\lambda')l_i(x)\rangle_{w_i}, \end{aligned} \tag{5}$$

Here, $\langle A(x)\rangle\equiv\int dx\,A(x)\rho(x)/\int dx\,\rho(x)$ denotes the equilibrium ensemble average with $\rho(x)$ the equilibrium distribution. The subscript denotes a conditional ensemble average and is defined as $\langle A(x)\rangle_\omega\equiv\int dx\,A(x)\omega(x)\rho(x)/\int dx\,\omega(x)\rho(x)$. The term $\langle\delta(\lambda(x)-\lambda')\rangle_{w_{i-1}}$ can be calculated by histogramming all time slices of the paths generated by the PPTIS algorithm in the interface $i-1$ ensemble. Similarly, $\langle\delta(\lambda(x)-\lambda')l_i\rangle_{w_i}$ can be obtained by histogramming the loop points of the trajectories in the ensemble of interface i. The remaining terms are computed by matching different histograms using scaling factors obtained from the overlapping regions between two windows. These scaling factors are here defined as $s_i\equiv\langle w_i(x)\rangle/\langle w_{i-1}(x)\rangle$ and follow, using Eqs. (3) and (4), from

$$s_i=\frac{\langle\delta(\lambda(x)-\lambda')b_{i-1}\rangle_{w_{i-1}}}{\langle\delta(\lambda(x)-\lambda')b_i\rangle_{w_i}}, \tag{6}$$

for any $\lambda', \lambda_{i-1}<\lambda'<\lambda_i$. Hence, one can integrate over λ' to obtain the most accurate value of s_i.

Using these scaling factors (6) and Eq. (5) one can derive the following relation for the relative probability of the order parameter values a and b with $\lambda_{i-1}<a<\lambda_i$ and $\lambda_i<b<\lambda_{i+1}$:

$$\frac{P(a)}{P(b)}=\frac{s_i^{-1}\langle\delta(\lambda(x)-a)\rangle_{w_{i-1}}+\langle\delta(\lambda(x)-a)l_i\rangle_{w_i}}{\langle\delta(\lambda(x)-b)\rangle_{w_i}+s_{i+1}\langle\delta(\lambda(x)-b)l_{i+1}\rangle_{w_{i+1}}}. \tag{7}$$

Hence, when all scaling factors s_i are known the total histogram $P(\lambda)$ can be computed by joining all probabilities from Eq. (7). Note that contrary to the rate calculation, the obtained free energy profile does not depend on the Markovian assumption introduced by PPTIS. Hence, this result is always exact, even when the memory loss requirement is not completely obeyed.

III. NUMERICAL RESULTS

We test the validity of the method on the dimer system already studied with TPS and TIS techniques [5,7,11]. We consider $N=100$ particles at fixed density in dimension $d=2$, interacting through a purely repulsive Weeks-Chandler-Andersen (WCA) potential. In addition, two of the particles experience a double well potential $V_{\text{dimer}}(r)$, with r the interparticle distance, so that its two minima correspond to the compact and extended configurations of a dimer (see Ref. [7] for details). The barrier height is chosen such that the states are stable, transitions between them are rare, and the rate constants are well defined. We chose 18 interfaces defined by the order parameter $\lambda=r$, the dimer interparticle distance. State A is defined by $r<\lambda_0$ and state B by $r>\lambda_{17}$. All system and PPTIS numerical parameters are identical to those in Secs. III A and III B of [7].

We considered two cases, one at constant temperature, and the other at constant energy. We first calculated the canonical free energy $\beta F(r)=-\ln P(r)$, at $T=1/\beta=0.755$, corresponding to the temperature in our previous free energy calculation [7]. In Fig. 3 we report the histograms of loop and boundary points for two consecutive PPTIS windows, together with the rescaling and rematching procedures. By iterating the procedure on all the windows, we computed the

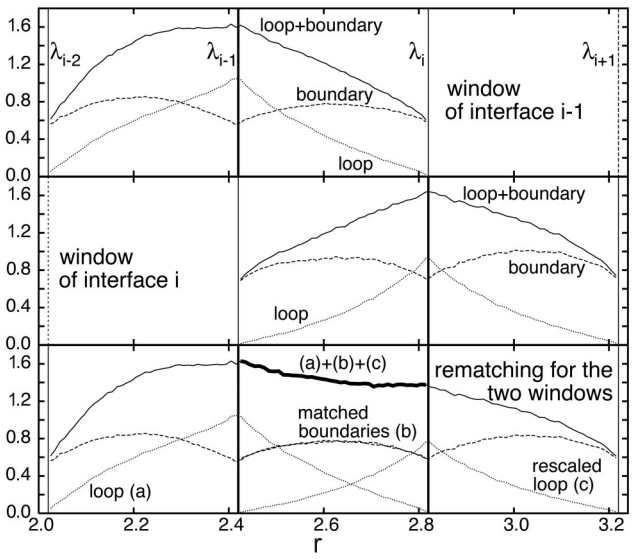

FIG. 3. The window rematching procedure. Top and middle panels: loop and boundary point histograms for two consecutive windows of the λ_{i-1} ensemble (with $\lambda_{i-2}=2.02<r<2.82=\lambda_i$) and the λ_i ensemble (with $\lambda_{i-1}=2.42<r<3.22=\lambda_{i+1}$). Bottom: construction of the corrected histogram $P(r)$ (thick solid line) between λ_{i-1} and λ_i. Repeating this procedure with windows λ_{i-2} and λ_{i+1} results in the probability histogram over the entire range $\lambda_{i-2}=2.02<r<3.22=\lambda_{i+1}$.

free energy between λ_1 and λ_{16}. The free energy in the stable regions A and B was obtained by directly histogramming $P(r)$ by means of two standard MC simulations. To check the PPTIS result we performed an independent MC free energy calculation. By applying a biasing potential of exactly $-V_{\mathrm{dimer}}(r)$ to the dimer system, one can simulate a system of pure WCA particles, and obtain the free energy from the probability of finding any two particles at distance r [7]. The resulting free energy agrees very well with our PPTIS results, as is shown in Fig. 4.

Path sampling simulations are often performed at constant energy. We therefore also performed a PPTIS simulation on the same system, at constant energy $E/N=1.0$, in order to compute the *NVE* free energy. Again, we checked the result

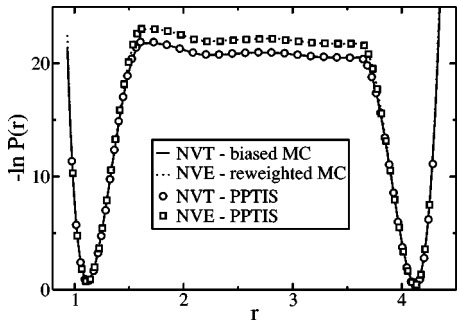

FIG. 4. Canonical and microcanonical free energies obtained from PPTIS and MC simulations. The errors are within the symbol size. The temperature and the energy of the respective *NVT* and *NVE* simulations were chosen to give the same average kinetic energy. Still, the free energy profile on top of the barrier is significantly different for the two ensembles.

TABLE I. PPTIS forward and backward rate constants k_{AB} and k_{BA}, as well as the equilibrium constant $C=k_{AB}/k_{BA}$. Moreover, integrating $P(r)$ from the free energy curves over the stable regions we can obtain their relative probabilities and the ratio C_F, which is another expression of the equilibrium rate. We also report C_{MC} obtained using the free energies from the biased MC simulations. The results are all consistent with each other.

	$k_{AB}/10^{-10}$	$k_{BA}/10^{-10}$	C	C_F	C_{MC}
NVT	10 ± 4	6 ± 2	1.5 ± 0.8	1.5 ± 0.2	1.419 ± 0.003
NVE	2.9 ± 0.5	1.9 ± 0.2	1.5 ± 0.3	1.39 ± 0.07	1.423 ± 0.002

by an independent free energy calculation. Using the constant temperature biased MC simulation described before, it is possible to reweight each canonical configuration to its proper microcanonical probability for the unbiased system. Let q,p be the dN-dimensional vectors of all positions and momenta, respectively. In the *NVT* ensemble the reduced configurational distribution for the biased system with total potential energy $V_{\mathrm{WCA}}(q)$ is $\rho_{\mathrm{can}}(q)\propto\exp[-\beta V_{\mathrm{WCA}}(q)]$. Instead, the microcanonical probability of the unbiased system that we need is

$$\rho_{\mathrm{mic}}(q)\propto\int dp\ \delta[H(q,p)-E]\delta(P)\propto[E-V_{\mathrm{WCA}}(q)-V_{\mathrm{dimer}}(r(q))]^{(dN-d-2)/2}, \tag{8}$$

where $H(q,p)$ is the Hamiltonian of the unbiased system, P is the d-dimensional vector of total momentum, and $r(q)$ is the dimer interparticle distance for a given configuration q. Applying the weight $\rho_{\mathrm{mic}}/\rho_{\mathrm{can}}$ for each MC configuration we can in a single simulation compute both *NVT* and *NVE* averages. As before, in the biased system it does not matter which two particles we consider as a dimer and we can increase the statistics averaging over all pairs. We report in Fig. 4 the *NVE* free energy profile obtained from the reweighted biased MC simulation together with the *PPTIS* one.

Finally, the forward and backward rate constants follow from a PPTIS simulation together with the free energy once the fluxes in (1) are known [5,7]. For both the canonical and microcanonical cases we computed f_A, f_B using MD trajectories with initial points in the stable states and sampled from the appropriate corresponding distribution. In Table I we report the final rates. The constant energy results compare well with our previous calculations [7].

IV. CONCLUSION

In conclusion, we have designed an algorithm that allows us to obtain the free energy profile within the PPTIS path sampling scheme. It is worth stressing that in traditional methods, such as the Bennett-Chandler procedure, first the free energy is computed and then the rates have to be determined in a separate simulation. Here, we have shown that a

method developed for rate computations also gives the free energy as a side product, with no additional computational effort. We believe that the loop-boundary method has many applications, e.g., in biomolecular simulations, where the calculation of free energy profiles is often done by means of MD, thus making the transition to PPTIS rather straightforward.

ACKNOWLEDGMENTS

We thank P. R. ten Wolde for a careful reading of the manuscript. T.S.v.E acknowledges the support of the Marie Curie Foundation (Grant No. MEIF-CT-2003-501976) within the Sixth European Community Framework Programme.

[1] C. H. Bennett, in *Algorithms for Chemical Computations*, edited by R. Christofferson, ACS Symposium Series No. 46 (American Chemical Society, Washington, DC, 1977).
[2] D. Chandler, J. Chem. Phys. **68**, 2959 (1978).
[3] D. Frenkel and B. Smit, *Understanding Molecular Simulation*, 2nd ed. (Academic Press, San Diego, CA, 2002).
[4] C. Dellago, P. G. Bolhuis, and P. L. Geissler, Adv. Chem. Phys. **123**, 1 (2002).
[5] T. S. van Erp, D. Moroni, and P. G. Bolhuis, J. Chem. Phys. **118**, 7762 (2003).
[6] P. G. Bolhuis, Proc. Natl. Acad. Sci. U.S.A. **100**, 12129 (2003).
[7] D. Moroni, P. G. Bolhuis, and T. S. van Erp, J. Chem. Phys. **120**, 4055 (2004).
[8] A. K. Faradjian and R. Elber, J. Chem. Phys. **120**, 10880 (2004).
[9] D. Moroni, Ph.D. thesis, University of Amsterdam, 2005.
[10] S. Duane, A. D. Kennedy, B. J. Pendleton, and D. Roweth, Phys. Lett. B **195**, 216 (1987).
[11] C. Dellago, P. G. Bolhuis, and D. Chandler, J. Chem. Phys. **110**, 6617 (1999).